Tanguy Mertens

A new mapped infinite partition of unity method for convected acoustical radiation in infinite domains.

January 20, 2009

Université Libre de Bruxelles

Remerciements

Si tu donnes un poisson à un homme, il ne mangera qu'un jour. S'il apprend à pêcher, il mangera toute sa vie.

Proverbe de Confucius, repris plus tard par Dominique Pire dans le cadre de l'action Iles de Paix.

Je remercie Philippe Bouillard de m'avoir donné ma canne à pêche et conduit à l'étang. Je remercie Laurent Hazard et Guy Paulus pour tous leurs conseils avisés. Et tous les autres, famille, amis, qui ont gardé confiance en moi et m'ont encouragé à la persévérance.

C'est grâce à vous tous que je peux vous présenter avec fierté mon premier poisson.

Ceci dit, je voudrais remercier de manière plus académique tous les acteurs du projet.

Je remercie Philippe Bouillard qui est à la source du projet et qui a contribué à mon épanouissement scientifique durant cette aventure au sein du service BATir. Je remercie également pour leur encadrement: Guy Warzée pour sa gentillesse et sa patience ainsi que Jean-Louis Migeot pour son soutien industriel et ses remarques pertinentes.

Ce passage au service BATir a été une expérience riche sur le plan scientifique mais aussi humain. Je remercie mes collègues de l'ULB pour les relations que nous avons construites ensemble, pour les activités dans le cadre du travail ou hors des murs de l'université. Je pense évidemment à Laurent Hazard et à Guy Paulus, pour leur amitié mais aussi leur disponibilité et leurs nombreux conseils. Merci aussi à tous les membres du service des milieux continus qui ont ajouté une dimension humaine. La nature des contrats de recherche et d'assistanat est tel qu'ils furent nombreux a être passés par les murs de l'université. Je ne pourrai tous les citer mais je tiens quand même à remercier personellement Katy, Erik, Geneviève, Yannick, Louise, Dominique, Thierry, Sandrine, Bertha, David, Benoît, Peter et Kfir.

S'il est vrai qu'un travail de thèse tend à rendre le chercheur autonome, les collaborations et interactions restent importantes. Je remercie à cet égard toute l'équipe de l'Institute of Sound and Vibration Research de l'université de Southampton. Je remercie Jeremy Astley, chef du service de m'y avoir accueilli pendant un stage de six mois. Je le

remercie aussi pour l'environnement de travail de qualité qu'il m'a offert. Il est évident que la présence de Pablo Gamallo à l'I.S.V.R. a énormément contribué à l'aboutissement de ce travail de recherche. Je le remercie pour tout le temps qu'il m'a consacré, à Southampton et même par la suite lors de contacts e-mail ou lors de rencontres en conférences. Je le remercie pour l'intérêt qu'il porte à la présente étude, pour ses encouragements et pour tous ses enseignements. Mais ce séjour n'a pas été que professionellement enrichissant, je repense à l'accueil qui m'a été réservé ainsi que de nombreux excellents souvenirs qui font de ce séjour une partie inoubliable de ma vie. Je tiens donc à remercier chaleureusement pour leur amitié précieuse Vincent et Theresa, Luigi, Claire, Naoki, Rie, Sue, Lisa, Eugene, Isa, Daniel et Stéphanie, Alessandro et Emmet.

Ces quelques lignes indiquent à quel point les relations humaines ont une influence sur ma vie. Cela ne sera pas une surprise alors si je remercie les personnes pour qui je *travaille dans les avions* ou ceux qui me félicitent de mon travail, *les semaines durant lesquelles, ils n'ont pas trop entendu les avions*. Je pense bien entendu à ma famille, principalement ma maman, pour avoir fait de moi l'homme que je suis aujourd'hui et mes amis, plus particulièrement mes collocataires: Iyad, Mathieu, Quentin, Guerrick, Caroline et Florence. Merci à vous de partager mes valeurs et de colorier mon existence.

Enfin, je terminerai par remercier les deux petits rayons de soleil qui ont ensoleillé la fin de ce long parcours.

List of Symbols

Greek symbols

β : $\sqrt{1 - M_0^2}$
γ : Poisson ratio of specific heat capacities : c_p/c_v
Γ : interface separating the inner and the outer domains
ε : Error
μ : phase function $[m]$
ρ : mass density $[kgm^{-3}]$
ρ_0 : steady mean density $[kgm^{-3}]$
ρ_a : acoustic density $[kgm^{-3}]$
$\boldsymbol{\sigma}$: stress tensor $[Nm^{-2}]$
ϕ : velocity potential $[m^2s^{-1}]$
ϕ_0 : mean velocity potential $[m^2s^{-1}]$
ϕ_a : acoustic velocity potential $[m^2s^{-1}]$
$\tilde{\phi}_a$: amplitude of the harmonic acoustic velocity potential $[m^2s^{-1}]$
$\tilde{\phi}^h$: numerical approximation of $\tilde{\phi}_a$ $[m^2s^{-1}]$
$\tilde{\phi}_h^I$: numerical approximation in the outer region Ω_o $[m^2s^{-1}]$
Φ_α : shape function for the α^{th} degree of freedom
Φ_α^I : infinite shape function for the α^{th} degree of freedom
ω : angular frequency $[s^{-1}]$
Ω : domain
Ω_i : inner region
Ω_o : outer region

Arabic symbols

$\tilde{a}_n$	: normal acceleration of a vibrating wall	$[ms^{-2}]$
A_n	: normal acoustic admittance	$[m^2skg^{-1}]$
$A_{mn}^{\pm}$	: incident and reflected modal amplitude	$[m^2s^{-1}]$
c	: speed of sound	$[ms^{-1}]$
c_0	: steady mean part of the speed of sound	$[ms^{-1}]$
c_∞	: speed of sound at large distance from the source	$[ms^{-1}]$
c_p	: specific heat capacity at constant pressure	$[JK^{-1}]$
c_v	: specific heat capacity at constant volume	$[JK^{-1}]$
$dofs$	: number of unknowns of the approximation	
E	: energy flow out of a surface	$[J]$
$E_{mn}^{\pm}$	: incident and reflected modal patern	
f	: excitation frequency	$[s^{-1}]$
G	: geometric factor	
h	: mesh size	$[m]$
H	: Hilbert space	
i	: imaginary unit $= \sqrt{-1}$	
$\mathbf{I}$	: Sound intensity	$[Wm^{-2}]$
J'	: stagnation entropy	$[Jkg^{-1}]$
k	: wavenumber	$[m^{-1}]$
$k_{r,mn}^{\pm}$	: incident and reflected radial wavenumber	$[m^{-1}]$
k_B	: Boltzmann constant	$[JK^{-1}]$
$K_{z,mn}^{\pm}$	: incident and reflected axial wavenumber	$[m^{-1}]$
L_j^d	: Legendre polynomial of order d for node j	
L_s	: curve enclosing the boundary S_s	
L_v	: curve enclosing the boundary S_v	
m	: angular mode number	
$\mathbf{m}'$	: mass flux	$[kgm^-2s^{-1}]$
m_0	: radial order of the infinite element	
m_w	: mass of a molecule	$[kg]$
M_0	: mach number	
M_i	: Mapping function for node/point i	
$\mathbf{n}$	: outer normal to the domain	
n	: radial mode number	
n_d^I	: number of infinite degree of freedom	
$n\,(j)$	: size of the local approximation space at node j	
nni	: number of infinite nodes	
$nodes$	: number of nodes	
N_i	: Partition of Unity function of node i	
N_m	: number of angular modes	
N_n	: number of radial modes	
N_M	: number of reflected modes (unknown)	

p	: fluid pressure	$[Pa]$
p_0	: steady mean fluid pressure	$[Pa]$
p_a	: acoustic pressure	$[Pa]$
$\tilde{p}_a$	: amplitude of the harmonic acoustic pressure	$[Pa]$
$\tilde{p}_{an}$	: analytic amplitude of the harmonic acoustic pressure	$[Pa]$
$\mathbf{q}$	: heat flux	$[Wm^{-2}]$
Q_w	: heat production	$[J]$
r_o	: distance to the source point	$[m]$
R	: specific gas constant	$[JK^{-1}mol^{-1}]$
R_j	: radial function for infinite node j	
R_j^d	: radial function of order d for node j	
s	: entropy	$[Jkg^{-1}K^{-1}]$
S	: boundary	
S_i	: mapping functions for the interface Γ	
S_M	: Modal boundary	
S_s	: soft wall	
S_v	: vibrating wall	
t	: time	$[s]$
T	: Temperature	$[K]$
T_j	: circumferential function for infinite node j	
$\tilde{u}_n$	: normal displacement of a vibrating wall	$[m]$
$\mathbf{v}$	: fluid velocity	$[ms^{-1}]$
$\mathbf{v}_0$	: steady mean fluid velocity	$[ms^{-1}]$
$\mathbf{v}_\infty$	: fluid velocity at large distance from the source	$[ms^{-1}]$
$\mathbf{v}_a$	: acoustic velocity	$[ms^{-1}]$
$\tilde{\mathbf{v}}_a$	: amplitude of the harmonic acoustic velocity	$[ms^{-1}]$
$\mathscr{V}$	: the Sobolev space $W^{1,2} = H^1 = \{f : f, \nabla f \in L^2\}$	
V_{jl}	: l^{th} local approximation function of node j	
$\tilde{w}_n$	: normal velocity of a vibrating wall	$[ms^{-1}]$
W_j	: weight function of node j	
W_j^I	: infinite weight function of the infinite node j	
$W_{M,nm}$	: modal weight function of the angular and radial mode (m, n)	

Operators

∇	: gradient operator
$\nabla\cdot$	: divergence operator
$\nabla\times$	: curl operator
Δ	: Laplacian operator
$\frac{D}{Dt}$	: Total time derivative
:	: the double dot product of two tensors
$\langle\ \rangle$	: time average
$\Re$	: Real part

Contents

7

Aliasing error

The aliasing error occurs for higher order Finite Element Method, never for the linear one. It only occurs at a particular number of degrees of freedom per wavelength. One interesting question is to know if the aliasing error also occurs in Partition of Unity Method. To answer this question more details have to be given on the origin of the aliasing error. This phenomenon can be explained theoretically with a dispersion analysis.

Let us consider an infinite, two-dimensional[1], periodic mesh. The distance along x between two elements is δx and δy along y. δx and δy are both taken equal to the internodal distance h.

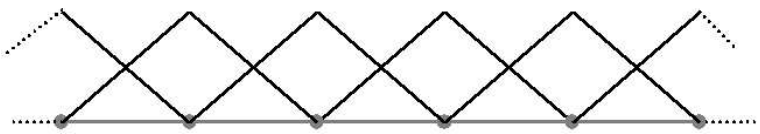

Fig. 7.1. Illustration of a one-dimensional mesh and linear shape functions.

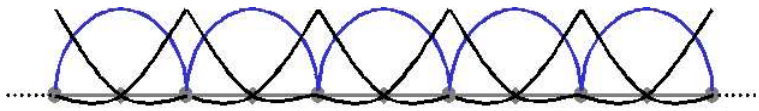

Fig. 7.2. Illustration of a one-dimensional mesh and quadratic shape functions.

We can identify N different types of nodes on the mesh. All nodes of a given type (p) share the same number of degrees of freedom (M_p) and are located at the same cyclically repeating position in the mesh pattern. This is illustrated for infinite propagation in a one-dimensional domain. The one-dimensional mesh (in grey) and shape functions are

[1] These results have been obtained by developing a two-dimensional convected Partition of Unity Method for inner cavities. This has not been detailed in this work but the formulation can be easily derived from the three-dimensional one.

plotted in figure 7.1 and 7.2 for the linear Finite Element Method and the quadratic one respectively. It can be easily noticed that it only exists one type of node in the linear case and two (vertices and mid-side nodes) types of nodes in the quadratic case.

As the mesh has a cyclic repeatability, the discrete finite element equations for a given scheme are identical for all nodes of a particular type. Therefore, a linear system for the unbounded problem is formed by N distinct types of equations:

$$\sum_{p=1}^{N} \sum_{m,n} A_{m,n}^{(q,p)} u_{m,n}^{(p)} = 0 \qquad for \quad q = 1, 2, ..., N \tag{7.1}$$

m, n are the position of the nodes in the grid, the matrix $A_{m,n}^{q,p}$ is obtained by the convected wave formulation (shape functions from node p and weight function from type node q) and $u_{m,n}^{(p)}$ the value of the nodal pressure of node type p at location $(m\delta x, n\delta y)$.

The wave solution can be expressed by equation 7.2 for a wave propagating in a direction given by the angle θ such that $k_x = kcos\,(\theta)$ and $k_y = ksin\,(\theta)$.

$$u_{m,n}^{(p)} = u_0^{(p)} e^{(ik_x \delta_x m)} e^{(ik_y \delta_y n)} \tag{7.2}$$

Each type of node generates a different set of equations. The unknowns are $\left\{u_0^{(p)}\right\}$ $(p = 1 : N)$ and correspond to the amplitude of the wave for type node p. This leads to a linear system $(RU = 0)$ which is the numerical dispersion relation of the model, where R is the dispersion matrix and U a vector containing all the unknowns $u_0^{(p)}$. When the wave direction θ is fixed, the system represents an eigenvalue problem for k and U. Non trivial solutions are obtained when the dispersion matrix is singular, we then look for $det\,(R) = 0$. This determinant is a polynome in K where $\left(K = e^{ikh}\right)$. The total number of roots $\left(\tilde{K}\ or\ \tilde{k}\right)$ is defined by the order of the polynomial. Dispersion analysis compares numerical roots $\tilde{k}$ and physical (prescribed) ones k.

A dispersion analysis has been done for a 'one-dimensional' $(\theta = \beta = 0)$ case by Gabard et al. [72] with free parameters M, k and h.

This analysis shows that the classical linear finite element method leads to only one type of nodes. The polynomial equation to solve is of order two [72]. It has two roots corresponding to the physical downstream and upstream propagations.

For quadratic finite elements, the polynome is of order four [72]. Among the four roots, two of them correspond to the physical upstream and downstream propagation. The two others are 'negative copies' of the physical roots. These roots correspond to $k^+ + (\pi/h)$ and $k^- + (\pi/h)$. As the interpollant is of the form $u_0(x) = u_0 e^{ikhm}$, a physical wavenumber and its negative copy can lead to the same interpolant at the nodes of the mesh (eq. 7.3). However, the continuous approximations are not identical.

$$\begin{aligned} u(x)|_{x=hm} &= u_0 e^{i\left(k^+ + \frac{\pi}{h}\right)hm} \\ &= u_0 e^{ik^+hm} e^{i\pi m} \\ &= \pm u_0 e^{ik^+hm} \end{aligned} \tag{7.3}$$

A problem arise for a given couple (k, h) when the correct downstream mode and a negative copy of the upstream mode have the same wavenumber $k^+ = k^- + (\pi/h)$. The numerical model can not then accommodate two modes with the same wavenumber but different eigenvectors $\tilde{U}$.

This analysis shows that the aliasing error only occurs for downstream convected propagation and for a particular combination of the mach number (M), the internodal distance (h) and the excitation frequency (f).

The following results illustrate the theory and show how aliasing affects the polynomial Partition of Unity Method. The first set of results corresponds to a pseudo one-dimensional application showing the effect of the flow on upstream and downstream wave propagation. Two-dimensional analysis are also performed to emphasize the behaviour of the computational method with respect to the orientation of the wave, the flow and the mesh.

7.1 One-dimensional case

The application which is considered here is the propagation of a plane wave within a uniform mean flow in the same or the opposite direction of the wave. Let us consider the wave traveling along x axis ($\theta = 0$) and the flow either along x ($\beta = 0$) or along $-x$ ($\beta = \pi$).

This can be modelled by a rectangular domain. Walls at $y = constant$ are considered as rigid walls. The plane wave is prescribed on boundaries at $x = constant$ by modal and transmitted boundary conditions.

The aim of this analysis is to illustrate the aliasing error. It means that we vary the number of degrees of freedom per wavelength and check the occurance of a peak of error.

As computations are made for upstream and downstream propagations with mach number varying from 0 to 1, results are compared on the number of degrees of freedom per physical wavelength ($2\pi/k_M h$ with k_M is the effective wavenumber obtained by taking into account the effect of the mean flow) and not the wavelength corresponding to the excitation frequency ($2\pi/kh$) with:

$$k_M = \frac{2\pi f}{c_0\left(1 + M cos\left(\beta\right)\right)} \tag{7.4}$$

The computational domain has been discretized by 10 elements along x and 10 along y. The wave is prescribed by modal and transmitted boundary conditions. The Finite Element and Partition of Unity Methods will be compared to results obtained by Gabard et al. [72].

To vary the number of degrees of freedom per wavelength, we vary the excitation frequency. This study has been made for mach number values from 0.1 to 0.9 in upstream and downstream propagations.

The enrichment of the Partition of Unity Method is of second order in x and y: $\{1, x^2, y^2\}$.

We can deduce that both Finite Element results (computed with a 'degenerated Partition of Unity Method' (figure 7.3) and those (figure 7.4) issued from paper [72]) are identical. The aliasing error does not have any influence on the classical Finite Element Method, as predicted by the theory.

The E_2 error corresponds to the mean of $\left|\tilde{p}_{an} - \tilde{p}^h\right| / \left|\tilde{p}_{an}\right|$ evaluated at each node of the domain.

While considering the Partition of Unity (figure 7.5) and the second order Finite Element (figure 7.6) results, we directly see the occurance of peaks of error. These peaks correspond to the aliasing error. They occur in the downstream propagation case with a mach number higher than 0.5. We can note that there only is one aliasing peak per mach number.

The Partition of Unity Method shows really good convergence rate compared to the other methods. This is due to the order of the enrichment and of the Partition of Unity shape functions.

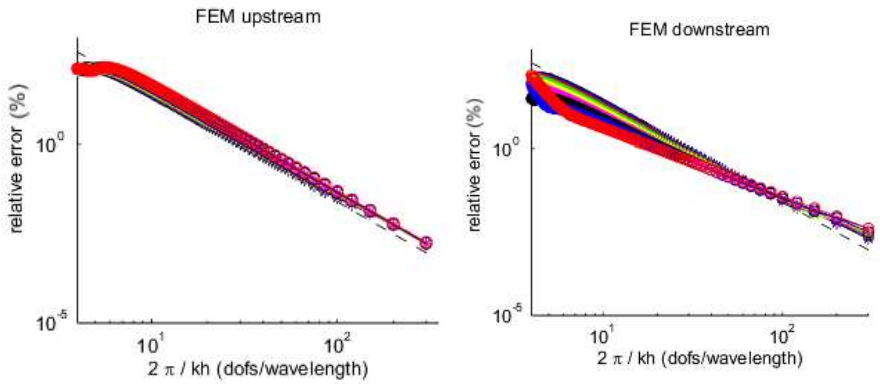

Fig. 7.3. Illustration of the aliasing (L^2 relative) error [%]: Finite Element computations (Partition of unity with the constant enrichment); upstream (left) and downstream (right) propagation (M=0.1 ($*$) to 0.9 (o)).

The results show that aliasing error is disturbing. As predicted by the theory, the aliasing error occurs for downstream propagation at larger number of degrees of freedom per

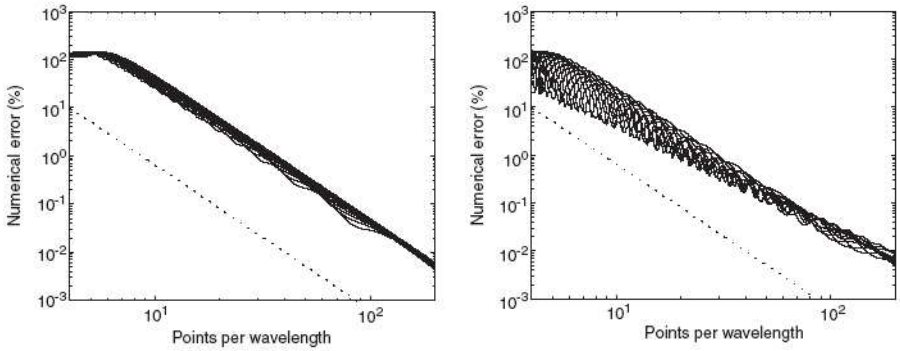

Fig. 7.4. Reproduced from [72]. Illustration of the aliasing (E_2) error : linear Finite Element results; upstream and downstream propagation (M=0.1 to 0.9).

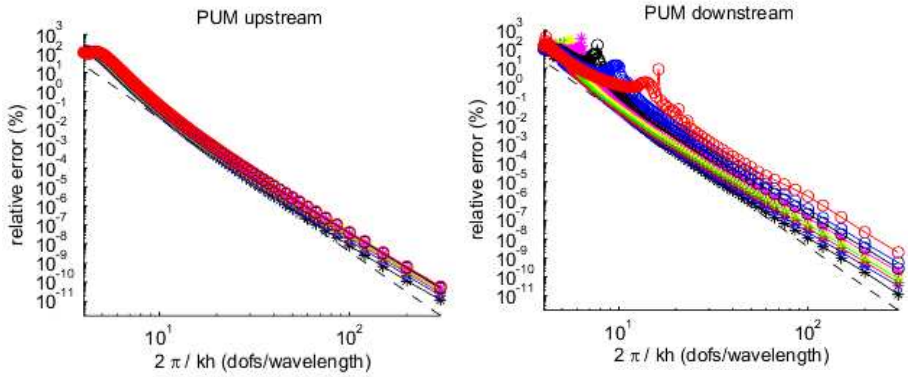

Fig. 7.5. Illustration of the aliasing error : Partition of Unity computations; upstream and downstream propagation (M=0.1 ($*$) to 0.9 (o)).

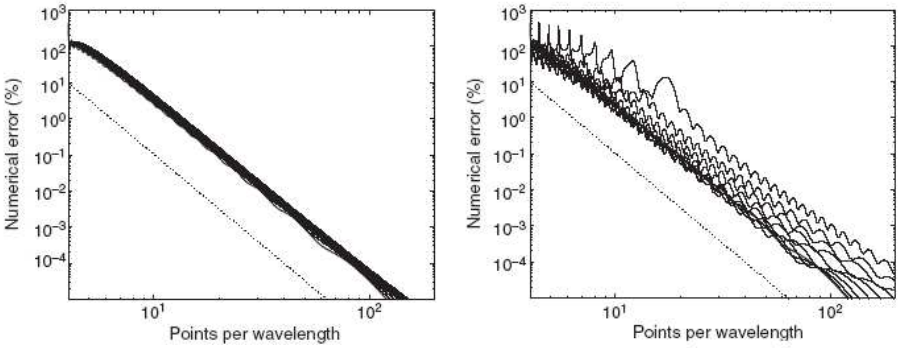

Fig. 7.6. Reproduced from [72]. Illustration of the aliasing error : Second order Finite Element results; upstream and downstream propagation (M=0.1 to 0.9).

wavelength than those prescribed by the rule of 6 to 10 degrees of freedom per wavelength. The range of Mach number where the aliasing error is disturbing corresponds to common values in turbofan applications.

7.2 Two-dimensional case

In this section, a two-dimensional analysis is performed to analyse the effect of the orientation of the flow (β) and the wave (θ) with respect to the orientation of the mesh. A plane wave propagates in a square computational domain. The wave is prescribed on the four boundaries with a mass flux rate boundary condition.

The (E_2) error for the partition of unity for $M = 0.8$ and using 17.7 degrees of freedom per wavelength, is plotted in the $\beta - \theta$ plane in figure 7.7. The enrichment used for the computation is proportional to $\{1, x^2, y^2\}$.

This result is compared with the figure 7.8 [73]. It corresponds to the dispersion error for the second order finite element for $M = 0.75$ and 10 degrees of freedom per wavelength.

Both figures show the same behaviour. The distribution of the dispersion error is dominated by isolated islands of errors while everywhere around the error is relatively low. These islands lie on the diagonal $\beta = \theta$ which corresponds to an alignment of the flow and the wave. However, the error peaks occur only in the vicinity of the x or y axes (i.e. $\beta = \theta = 0, \pi/2, \pi, 3\pi/2$).

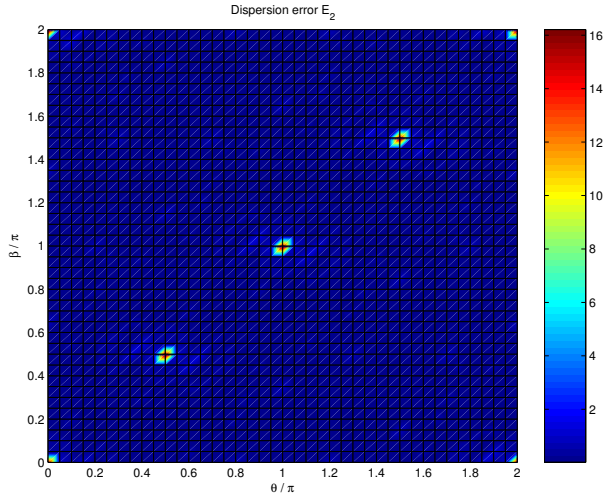

Fig. 7.7. Dispersion error E_2 in function of θ and β with partition of unity for $M = 0.8$ and 17.7 degrees of freedom per wavelength .

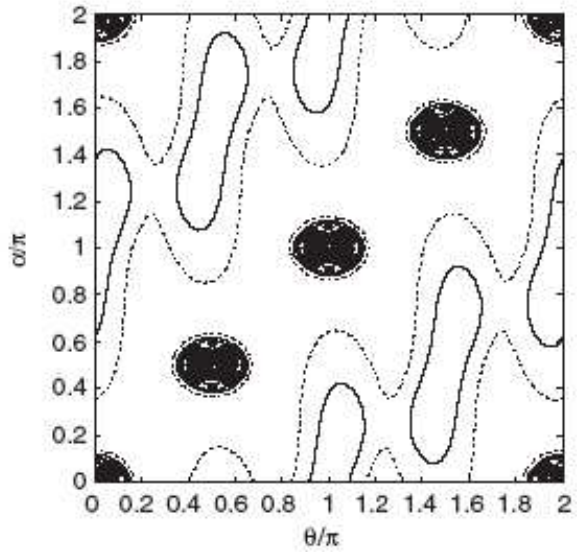

Fig. 7.8. Reproduced from [73]. E_2 error in function of θ and β with second order finite element for $M = 0.75$ and 10 degrees of freedom per wavelength (E_2 varying from 0.1 to 1.5%).

The conclusions from Gabard [73] for the convected Finite Element Method are also valid for the Partition of Unity Method. Indeed, we also observed that the aliasing error only occurs when the flow, the mesh and the wave are aligned. All three conditions are required. This remark can be used in applications. If for example the flow is not aligned with the mesh, this error will not occur. Since in general, the direction of the flow can be computed before acoustic computations, aliasing error will not occur if the mesh is constructed so that it is not aligned with the flow.

References

1. Ph. Bouillard, F. Ihlenburg, Error estimation and adaptivity for the finite element solution in acoustics: 2D and 3D applications, Comput. Methods Appl. Mech. Engrg. 176 (1999) 147-163.
2. F. Ihlenburg, I. Babuška, Dispersion analysis and error estimation of Galerkin finite element methods for the Helmholtz equation, Int. J. Numer. Methods Eng. 38 (1995) 3745-3774.
3. J.T. Oden, S. Prudhomme, L. Demkowicz, A posteriori error estimation for acoustic wave propagation problems, Arch. Comput. Meth. Engng. 12 (2005) 343-389.
4. F. Ihlenburg, I. Babuška, Finite element solution of the Helmholtz equation with high wave number part II : the h-p version of the FEM, SIAM J. Numer. Anal. 34 (1997) 315-358.
5. O.C. Zienkiewicz, Achievements and some unsolved problems of the finite element method, Int. J. Numer. Methods Eng. 47 (2000) 9-28.
6. L.L. Thompson, A review of finite element methods for time-harmonic acoustics, J. Acoust. Soc. Am. 119 (2006) 1315-1330.
7. J.M. Melenk, I. Babuška, The partition of unity finite element method: basic theory and applications, Comput. Methods Appl. Mech. Engrg. 139 (1996) 289-314.
8. I. Babuška, J.M. Melenk, The Partition of Unity Method, Int. J. Numer. Methods Eng. 40 (1997) 727-758.
9. O. Laghrouche, P. Bettess, R. J. Astley, Modeling of short wave diffraction problems using approximating systems of plane waves, Int. J. Numer. Methods Eng. 54 (2002) 1501-1533.
10. Th. Strouboulis, I. Babuška, R. Hidajat, The generalized finite element method for Helmholtz equation: Theory, computation, and open problems, Comput. Methods Appl. Mech. Engrg. 195 (2006) 4711-4731.
11. Th. Strouboulis, R. Hidajat, I. Babuška, The generalized finite element method for Helmholtz equation Part II: Effect of choice of handbook functions, error due to absorbing boundary conditions and its assessment, Comput. Methods Appl. Mech. Engrg. 197 (2008) 364-380.
12. Th. Strouboulis, K. Copps, I. Babuška, The generalized finite element method, Comput. Methods Appl. Mech. Engrg. 190 (2001) 4081-4193.
13. Th. Strouboulis, I. Babuška, K. Copps, The design and analysis of the generalized finite element method, Comput. Methods Appl. Mech. Engrg. 181 (2000) 43-69.
14. C. Farhat, I. Harari, L.P. Franca, The discontinuous enrichment method, Comput. Methods Appl. Mech. Engrg. 190 (2001) 6455-6479.
15. B. Pluymers, W. Desmet, D. Vandepitte, P. Sas, Application of an efficient wave-based prediction technique for the analysis of vibro-acoustic radiation problems, J. Comput. Appl. Math. 168 (2004) 353-364.
16. P. Gamallo, R.J. Astley, A comparison of two Trefftz-type methods: The ultraweak variational formulation and the least-squares method, for solving shortwave 2-D Helmholtz problems, Int. J. Numer. Methods Eng. 71 (2007) 406-432.
17. P. Gamallo, R.J. Astley, The partition of unity finite element method for short wave acoustic propagation on non-uniform potential flows, Int. J. Numer. Methods Eng. 65 (2006) 425-444.
18. T. Huttunen, P. Gamallo, R.J. Astley, Comparison of two wave element methods for the Helmholtz problem, Commun. Numer. Meth. Engng. Article in Press (2008) doi:10.1002/cnm1102.
19. T. Huttunen, P. Monk, J.P. Kaipio, Computational aspects of the ultra weak variational formulation, J. Comput. Phys. 182 (2002) 27-46.
20. T. Huttunen, J.P. Kaipio, P. Monk, An ultra weak method for acoustic fluid-solid interaction, J. Comput. Appl Math. 213 (2008) 166-185.

21. P. Monk, D.-Q. Wang, A least squares method for the Helmholtz equation, Comput. Methods Appl. Mech. Engrg. 175 (1999) 121-136.
22. R. Sevilla, S. Fernández-Méndez, A. Huerta, NURBS-enhanced finite element method (NEFEM), Int. J. Numer. Methods Eng. Early ViewW (2008) doi: 10.1002/nme.2311
23. E. Chadwick, P. Bettess, O. Laghrouche, Diffraction of short waves modeled using new mapped wave envelope finite and infinite elements, Int. J. Numer. Methods Eng. 45 (1999) 335-354.
24. E. De Bel, P. Villon, Ph. Bouillard, Forced vibrations in the medium frequency range solved by a partition of unity method with local information, Int. J. Numer. Methods Eng. 162 (2004) 1105-1126.
25. L. Hazard, Ph. Bouillard, Structural dynamics of viscoelastic sandwich plates by the partition of unity finite element method, Comput. Methods Appl. Mech. Engrg. 196 (2007) 4101-4116.
26. T.J.R. Hughes, J.A. Cotrell, Y. Bazilevs, Isogeometric analysis: CAD, finite elements, NURBS, exact geometry and mesh refinement, Comput. Methods Appl. Mech. Engrg. 194 (2005) 4135-4195.
27. B. Szabó, A. Düster, E. Rank, The p-version of the finite element method, in: E. Stein, R. de Borst, T.J.R. Hughes (Eds.), Fundamentals, Encyclopedia of Computational Mechanics, vol. 1, Wiley, New York, 2004 (Chapter 5).
28. R.J. Astley, P. Gamallo, Special short wave elements for flow acoustics, Comput. Methods Appl. Mech. Engrg. 194 (2005) 341-353.
29. R.J. Astley, P. Gamallo, The Partition of Unity Finite Element Method for Short Wave Acoustic Propagation on Non-uniform Potential Flows, Int. J. Numer. Methods Eng. 65 (2006) 425-444.
30. R.J. Astley, G.J. Macaulay, J.-P. Coyette, L. Cremers, Three-dimensional wave-envelope elements of variable order for acoustic radiation and scattering. Part I. Formulation in the frequency domain, J. Acoust. Soc. Am. 103 (1998) 49-63.
31. R.J. Astley, J.-P. Coyette, Conditioning of infinite element schemes for wave problems, Commun. Numer. Meth. Engng. 17 (2001) 31-41.
32. D. Dreyer, O. von Estorff, Improved conditioning of infinite elements for exterior acoustics, Int. J. Numer. Methods Eng. 58 (2003) 933-953.
33. J.J. Shirron, I. Babuška, A comparison of approximate boundary conditions and infinite element methods for exterior Helmholtz problems, Comput. Methods Appl. Mech. Engrg. 164 (1998) 121-139
34. D. Dreyer, Efficient infinite elements for exterior acoustics, PhD thesis, Shaker Verlag, Aachen, 2004.
35. W. Eversman, Mapped infinite wave envelope elements for acoustic radiation in a uniformly moving medium, J. Sound Vib. 224 (1999) 665-687.
36. S.J. Rienstra, W. Eversman, A numerical comparison between the multiple-scales and finite-element solution for sound propagation in lined flow ducts, J. Fluid Mech. 437 (2001) 367-384.
37. S.J. Rienstra, Sound transmission in slowly varying circular and annular lined ducts with flow, J. Fluid Mech. 380 (1999) 279-296.
38. S.J. Rienstra, The Webster equation revisited, 8th AIAA/CEAS Aeroacoustic conference (2002) AIAA 2002-2520.
39. M.K. Myers, On the acoustic boundary condition in the presence of flow, J. Sound Vib. 71 (1980) 429-434.
40. T. Mertens, Meshless modeling of acoustic radiation in infinite domains, Travail de spécialisation, Université Libre de Bruxelles (U.L.B.), 2005.
41. W. Eversman, The boundary condition at an impedance wall in a non-uniform duct with potential mean flow, J. Sound Vib. 246 (2001) 63-69.
42. B. Regan, J. Eaton, Modeling the influence of acoustic liner non-uniformities on duct modes, J. Sound Vib. 219 (1999) 859-879.
43. H.-S. Oh, J.G. Kim, W.-T. Hong, The Piecewise Polynomial Partition of Unity Functions for the Generalized Finite Element Methods, Comput. Methods Appl. Mech. Engrg. Accepted manuscript (2008), doi: 10.1016/j.cma.2008.02.035.
44. Free Field Technologies, Actran user's manual, http://fft.be.
45. University of Florida, Department of Computer and Information Science and Engineering, http://www.cise.ufl.edu/research/sparse/umfpack/
46. T.A. Davis, A column pre-ordering strategy for the unsymmetric-pattern multifrontal method, ACM Transactions on Mathematical Software 30 (2004) 165-195.
47. T.A. Davis, Algorithm 832: UMFPACK, an unsymmetric-pattern multifrontal method, ACM Transactions on Mathematical Software 30 (2004) 196-199.
48. T.A. Davis and I.S. Duff, A combined unifrontal/multifrontal method for unsymmetric sparse matrices, ACM Transactions on Mathematical Software 25 (1999) 1-19.

49. T.A. Davis and I.S. Duff, An unsymmetric-pattern multifrontal method for sparse LU factorization, SIAM Journal on Matrix Analysis and Applications 18 (1997) 140-158.
50. A. Hirschberg, S.W. Rienstra, An introduction to aeroacoustics, Eindhoven University of Technology (2004).
51. G. Warzée, Mécanique des solides et des fluides, Université Libre de Bruxelles (2005).
52. M.J. Crocker, Handbook of acoustics, Wiley-Interscience, New York (1998).
53. R. Sugimoto, P. Bettess, J. Trevelyan, A numerical integration scheme for special quadrilateral finite elements for the helmholtz equation, Commun. Numer. Meth. Engng. 19 (2003) 233-245.
54. G. Gabard, R.J. Astley, A computational mode-matching approach for sound propagation in three-dimensional ducts with flow, J. Sound Vib. Article in Press (2008) doi:10.1016/j.jsv.2008.02.015.
55. C. Farhat, I. Harari, U. Hetmaniuk, A discontinuous Galerkin method with Lagrange multipliers for the solution of Helmholtz problems in the mid-frequency regime, Comput. Methods Appl. Mech. Engrg. 192 (2003) 1389-1419.
56. C.L. Morfey, Acoustic energy in non-uniform flows, J. Sound Vib. 14 (1971) 159-170.
57. F. Magoules, I. Harari (editors), Special issue on Absorbing Boundary Conditions, Comput. Methods Appl. Mech. Engrg. 195 (2006) 3354-3902.
58. M. Fischer, U. Gauger, L. Gaul, A multipole Galerkin boundary element method for acoustics, Engineering Analysis with Boundary Elements 28 (2004) 155-162.
59. J.-P. Bérenger, Three-dimensional Perfectly Matched Layer for the absorption of electromagnetic waves, J. Comput. Phys. 127 (1996) 363-379.
60. C. Michler, L. Demkowicz, J. Kurtz, D. Pardo, Improving the performance of Perfectly Matched Layers by means of hp-adaptivity, Numerical Methods for Partial Differential Equations 23 (2007) 832-858.
61. A. Bayliss, E. Turkel, Radiation boundary conditions for wave-like equations, Comm. Pure Appl. Math. 33 (1980) 707-725.
62. B. Engquist, A. Majda, Radiation boundary conditions for acoustic and elastic wave calculations, Comm. Pure Appl. Math. 32 (1979) 313-357.
63. K. Feng, Finite element method and natural boundary reduction, Proceedings of the International Congress of Mathematicians, Warsaw (1983) 1439-1453.
64. D. Givoli, B. Neta, High-order non-reflecting boundary scheme for time-dependent waves, J. Comput. Phys. 186 (2003) 24-46.
65. T. Hagstrom, A. Mar-Or, D. Givoli, High-order local absorbing conditions for the wave equation: Extensions and improvements, J. Comput. Phys. 227 (2008) 3322-3357.
66. T. Hagstrom, T. Warburton, A new auxiliary variable formulation of high-order local radiation boundary conditions: corner compatibility conditions and extensions to first order systems, Wave Motion 39 (2004) 327-338.
67. A. Hirschberg, S.W. Rienstra, An introduction to aeroacoustics, Eindhoven university of technology (2004).
68. V. Lacroix, Ph. Bouillard, P. Villon, An iterative defect-correction type meshless method for acoustics, Int. J. Numer. Meth. Engng 57 (2003) 2131-2146.
69. T. Mertens, P. Gamallo, R. J. Astley, Ph. Bouillard, A mapped finite and infinite partition of unity method for convected acoustic radiation in axisymmetric domains, Comput. Methods Appl. Mech. Engrg. 197 (2008) 4273-4283.
70. G. Gabard, Discontinuous Galerkin methods with plane waves for time harmonic problems, J. Comput. Phys. 225 (2007) 1961-1984.
71. L. Hazard, Design of viscoelastic damping for vibration and noise control: modeling, experiments and optimisation, PhD thesis, Univesité Libre de Bruxelles (2007).
72. G. Gabard, R.J. Astley, M. Ben Tahar, Stability and accuracy of finite element methods for flow acoustics. I: general theory and application to one-dimensional propagation, Int. J. Numer. Meth. Eng. 63, (2005) 947-973.
73. G. Gabard, R.J. Astley, M. Ben Tahar, Stability and accuracy of finite element methods for flow acoustics. II: Two-dimensional effects, Int. J. Numer. Meth. Eng. 63 (2005) 974-987.
74. A. Goldstein, Steady state unfocused circular aperture beam patterns in non attenuating and attenuating fluids, J. Acoust. Soc. Am. 115 (2004) 99-110.
75. T. Douglas Mast, F. Yu, Simplified expansions for radiation from baffled circular piston, J. Acoust. Soc. Am. 118 (2005) 3457-3464.
76. T. Hasegawa, N. Inoue, K Matsuzawa, A new rigorous expansion for the velocity potential of a circular piston source, J. Acoust. Soc. Am. 74 (1983) 1044-1047.
77. R.J. Astley, A finite element, wave envelope formulation for acoustical radiation in moving flows, J. Sound Vib. 103 (1985) 471-485.
78. J.M. Tyler, T.G. Sofrin, Axial flow compressor noise studies, SAE Transactions 70 (1962) 309-332.

79. M.C. Duta, M.B. Giles, A three-dimensional hybrid finite element/spectral analysis of noise radiation from turbofan inlets, J. Sound Vib. 296 (2006) 623-642.
80. H.H. Brouwer, S.W. Rienstra, Aeroacoustics research in Europe: The CEAS-ASC report on 2007 highlights, J. Sound Vib. Article in Press (2008) doi:10.1016/j.jsv.2008.07.020.
81. http://en.wikipedia.org/wiki/Aircraft_noise, 4th September 2008.
82. Y. Park, S. Kim, S. Lee, C. Cheong, Numerical investigation on radiation characteristics of discrete-frequency noise from scarf and scoop aero-intakes, Appl. Acoust. Article in press (2008) doi:10.1016/j.apacoust.2007.09.005.
83. General Electric Company, http://www.ge.com, http://www.turbokart.com/about_ge90.htm, 4th September 2008.
84. R.J. Astley, J.A. Hamilton, Modeling tone propagation from turbofan inlets - The effect of extended lip liner, AIAA paper 2002-2449 (2002).
85. V. Decouvreur, Updating acoustic models: a constitutive relation error approach, PhD thesis, Université Libre de Bruxelles (2008).
86. P.A. Nelson, O. Kirkeby, T. Takeuchi, and H. Hamada, Sound fields for the production of virtual acoustic images, Letters to the editor, J. Sound Vib. 204 (1999) 386-396.
87. Y. Reymen, W. De Roeck , G. Rubio, M. Bealmans, W. Desmet, A 3D Discontinuous Galerkin Method for aeroacoustic propagation, Proceedings of the 12th International Congress on Sound and Vibration 2005.
88. G. Gabard, Exact integration of polynomial-exponential products with an application to wave based numerical methods, Commun. Numer. Meth. Engng (2008) doi: 10.1002/cnm.1123.
89. New York University, http://math.nyu.edu/faculty/greengar/shortcourse_fmm.pdf, 1st december 2008.